

XXVIIth International Conference on Ultrarelativistic Nucleus-Nucleus Collisions  
(Quark Matter 2018)

## Towards the equation of state at finite density from the lattice

Szabolcs Borsanyi,<sup>a</sup> Zoltan Fodor,<sup>a,b,c</sup> Jana N. Guenther<sup>a,d</sup>, Sandor K. Katz,<sup>d</sup>  
Attila Pasztor,<sup>a</sup> Israel Portillo,<sup>c</sup> Claudia Ratti<sup>c</sup>, K. K. Szabó,<sup>a,c</sup><sup>a</sup>University of Wuppertal, Department of Physics, Wuppertal D-42097, Germany<sup>b</sup>Eötvös University, Budapest 1117, Hungary<sup>c</sup>Jülich Supercomputing Centre, Jülich D-52425, Germany<sup>d</sup>University of Regensburg, Department of Physics, Regensburg D-93053, Germany<sup>e</sup>Department of Physics, University of Houston, Houston, TX 77204, USA

---

**Abstract**

A new precision lattice simulation set is analyzed for the equation of state to sixth order. We used lattice results at imaginary chemical potentials to calculate the Taylor coefficients, from which the pressure, trace anomaly, energy and entropy density as well as the baryon number can be derived. We discuss an alternative extrapolation strategy and show first results for zero strangeness chemical potential.

**Keywords:** Equation of state, lattice QCD

---

**1. Introduction**

The equation of state of the strongly interacting matter has been calculated from first principles by lattice QCD [1, 2]. The dynamical effect of the charm quark was calculated in [3]. While at LHC energies these results are satisfactory, for RHIC physics one has to extend the range of the computations to finite densities. For lattice QCD this is a very difficult task, since the simulated action turns complex when a baryo-chemical potential is introduced. A remedy for this situation is the calculation of the Taylor expansion coefficients of e.g. the pressure that represents a small parameter expansion in  $\mu_B/T$  [4, 5]. Similar expansion  $\mu_B/T$  is also possible for the transition temperature [6, 7]. In the Beam Energy Scan II program the expansion parameter  $\mu_B/T$  can be as large as 4 at chemical freeze-out, but individual fluid cells can have even higher chemical potentials [8].

Apart from the zero chemical potential, imaginary values are equally unproblematic to simulate [9, 10, 11]. The transition line [12, 13, 6], fluctuations [14] and the equation of state [15] have been calculated by studying the chemical potential dependence of thermodynamic observables, such as the chiral condensate, or, the (imaginary) baryon and other charge densities. The observed dependence on the (imaginary) chemical potential can be used to extrapolate to real chemical potentials using the analytic nature of the transition [16].

## 2. Taylor coefficients from imaginary $\mu_B$

Recently we have calculated high order baryon fluctuations on an  $N_t = 12$  lattice using imaginary- $\mu_B$  chemical potentials. Most importantly, we determined the

$$\chi_n^B(T, \hat{\mu}_B) = \left. \frac{\partial^n (p/T^4)}{(\partial \hat{\mu}_B)^n} \right|_T \quad (1)$$

with  $\hat{\mu}_B = \mu_B/T$  for several temperatures as well as imaginary values of the chemical potential  $0 \leq \text{Im } \hat{\mu}_B < \pi$ . All these simulations can be described by the global pressure function:

$$\chi_0^B(\hat{\mu}_B) = c_0 + c_2 \hat{\mu}_B^2 + c_4 \hat{\mu}_B^4 + c_6 \hat{\mu}_B^6 + c_8 \hat{\mu}_B^8 + c_{10} \hat{\mu}_B^{10} + \dots, \quad (2)$$

where  $c_n$  are the (temperature dependent) Taylor coefficients for the equation of state:  $n!c_n = \chi_n^B(T, \hat{\mu}_B = 0)$ . We keep the truncated series up to  $c_{10}$  order. We extract the  $\chi_1^B(T, \hat{\mu}_B), \dots, \chi_4^B(T, \hat{\mu}_B)$  quantities from each simulation and fit these as a function of  $\hat{\mu}_B$  with the corresponding derivative of Eq. (2). For  $c_8$  and  $c_{10}$  we introduce priors to stabilize the fit. For the details of the correlated fit over all our ensembles at a given temperature  $T$  see Ref. [17]. Results at different temperatures are not correlated. The fit coefficients  $\chi_{2n}^B(T, \hat{\mu}_B = 0)$  we plot in Fig. 1.

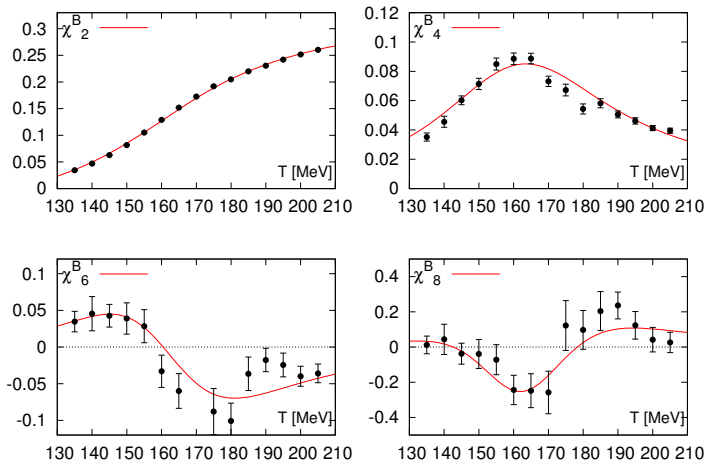


Fig. 1. Results for  $\chi_2^B, \chi_4^B, \chi_6^B$  and an estimate for  $\chi_8^B$  as functions of the temperature, obtained from the single-temperature analysis. The  $\chi_8^B$  determination was guided by a prior (see [17]). The red curve in each panel corresponds to a simple analytical estimate.

## 3. Analytical estimate

The pattern in Fig. 1 can be understood as the consequence of a  $\mu_B$  dependent transition temperature. To illustrate this we plotted the baryon density, normalized to  $\hat{\mu}_B$  for zero and an imaginary chemical potential in the left panel of Fig. 2. The shifting of  $T_c$  is numerically given by the  $\kappa$  curvature of the phase diagram, which we take from Ref. [18]. Using this  $\kappa$  coefficient to rescale the temperature axis by  $(1 - \kappa \hat{\mu}_B^2)$  we find that the rescaled  $\mu_B = 0$  curve well reproduces our direct lattice result at imaginary  $\mu_B$ .

Turning this observation into an ansatz, we can now model  $\chi_B/\hat{\mu}_B(T, \hat{\mu}_B)$  using the given  $\kappa$  coefficient and our  $\chi_B^2$  result from the first panel of Fig. 1. These assumed functions can be analyzed for their  $\hat{\mu}_B$

dependence at fixed  $T$  and the Taylor coefficients can be calculated. The resulting curves are shown and compared to the lattice results in red in Fig. 1. For such a simple ansatz the agreement is remarkable.

What do we learn from the approximate agreement between the analytic estimate and the lattice result? If this simple ansatz was exact, the baryon density could also be extended to real finite density. Since the strength of the transition is  $\mu_B$ -independent in this construction this ansatz assumes the absence of a critical end point. As long as a lattice simulation is consistent with this simple ansatz, it is also consistent with the scenario without a critical end point.

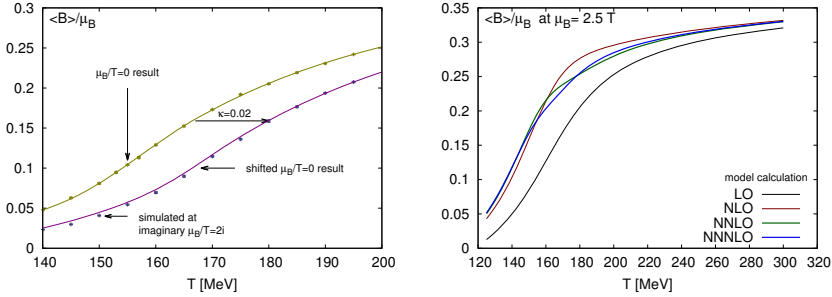


Fig. 2. Left:  $\chi_1^B(T, \hat{\mu}_B)$  as a function of the temperature for zero and a typical fixed imaginary  $\hat{\mu}_B$  value. The inflection point marks the transition, which is at a higher temperature for imaginary  $\hat{\mu}_B$ . The imaginary  $\hat{\mu}_B$  result (blue error bars) is very close to the shifted  $\mu_B = 0$  result (violet curve). Right: Using the analytical estimates for  $\chi_n^B$  as Taylor coefficients we extrapolated to  $\hat{\mu}_B = 2.5$  and plotted the baryon density. The truncation of the Taylor series introduces artificial inflection points.

#### 4. Alternative extrapolation

Having a high order Taylor expansion of the pressure does not necessarily gives an accurate description of the equation of state. In the right panel of Fig. 2 we show four truncations of the Taylor series. Keeping only  $\chi_2^B$  (LO) or  $\chi_4^B$  (NLO) the results are plausible. However, higher orders introduce “wiggles” that might destabilize the hydrodynamic application where it is used. The reason for this behaviour is the oscillatory pattern of high  $\chi_n^B$  coefficients, which in turn, is caused by the  $\mu_B$  dependent transition temperature. In the transition region these coefficients must extrapolate from the deconfined phase to the confined phase, or the other way around, depending on the used sign of  $\mu_B^2$ .

A less problematic prescription could be obtained if the extrapolation did not cross phase boundaries. Fig. 3 shows an example for such an extrapolation. We connect the points on the QCD phase diagram with equal  $\chi_1^B(T, \hat{\mu}_B)/\hat{\mu}_B$  values and extrapolate these to  $\hat{\mu}_B > 0$  using a low order polynomial or a rational function. The contours (once continuum extrapolated) can be used to determine  $\chi_1^B(T, \mu_B)$  at  $\mu_B > 0$ . For this we also need the already continuum extrapolated  $\chi_2^B$  (see Ref. [19]) that associates values to the contour lines. Here we show results for three lattice spacings, that are lying on top of each other. The extrapolation, however, introduces significant systematical errors beyond  $\hat{\mu}_B > 2$ , which requires further studies.

**Acknowledgements:** This project was funded by the DFG grant SFB/TR55. This work was supported by the Hungarian National Research, Development and Innovation Office, NKFIH grants KKP126769 and K113034. An award of computer time was provided by the INCITE program. This research used resources of the Argonne Leadership Computing Facility, which is a DOE Office of Science User Facility supported under Contract DE-AC02-06CH11357. The authors gratefully acknowledge the Gauss Centre for Supercomputing e.V. ([www.gauss-centre.eu](http://www.gauss-centre.eu)) for funding this project by providing computing time on the GCS Supercomputer JUQUEEN[20] at Jülich Supercomputing Centre (JSC) as well as on HAZELHEN at HLRS Stuttgart, Germany. This material is based upon work supported by the National Science Foundation under grants no. PHY-1654219 and OAC-1531814 and by the U.S. Department of Energy, Office of Science,

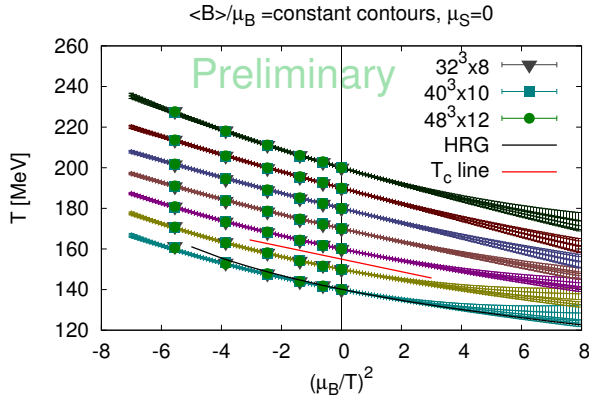


Fig. 3. Contours of fixed baryon-density-over-chemical-potential ratios on the QCD phase diagram. On the left hand side lattice simulations at imaginary chemical potentials constrain the contours, which are extrapolated to real chemical potentials on the right hand side. The contour at  $T_c$  is consistent with the curvature of the transition line.

Office of Nuclear Physics, within the framework of the Beam Energy Scan Theory (BEST) Topical Collaboration. C.R. also acknowledges the support from the Center of Advanced Computing and Data Systems at the University of Houston.

## References

- [1] S. Borsanyi, et al., Full result for the QCD equation of state with 2+1 flavors, *Phys.Lett. B* 730 (2014) 99–104. arXiv:1309.5258,
- [2] A. Bazavov, et al., Equation of state in (2+1)-flavor QCD, *Phys.Rev. D* 90 (9) (2014) 094503. arXiv:1407.6387,
- [3] S. Borsanyi, et al., *Nature* 539 (7627) (2016) 69–71. arXiv:1606.07494,
- [4] S. Borsanyi, et al., QCD equation of state at nonzero chemical potential: continuum results with physical quark masses at order  $m\mu^2$ , *JHEP* 1208 (2012) 053. arXiv:1204.6710,
- [5] A. Bazavov, et al., The QCD Equation of State to  $O(\mu_B^6)$  from Lattice QCD, *Phys. Rev. D* 95 (5) (2017) 054504. arXiv:1701.04325,
- [6] C. Bonati, M. D’Elia, F. Negro, F. Sanfilippo, K. Zambello, Curvature of the pseudocritical line in QCD: Taylor expansion matches analytic continuation, *Phys. Rev. D* 98 (5) (2018) 054510. arXiv:1805.02960,
- [7] P. Steinbrecher, The QCD crossover at zero and non-zero baryon densities from Lattice QCD arXiv:1807.05607.
- [8] S. A. Bass, et al. Probing the QCD Critical Point with Relativistic Heavy-Ion Collisions, *Central Eur. J. Phys.* 10 (2012) 1278–1281. arXiv:1202.0076,
- [9] Z. Fodor, S. Katz, *Phys.Lett. B* 534 (2002) 87–92. arXiv:hep-lat/0104001,
- [10] P. de Forcrand, O. Philipsen, The QCD phase diagram for small densities from imaginary chemical potential, *Nucl.Phys. B* 642 (2002) 290–306. arXiv:hep-lat/0205016,
- [11] M. D’Elia, F. Di Renzo, M. P. Lombardo, The Strongly interacting quark gluon plasma, and the critical behaviour of QCD at imaginary  $\mu$ , *Phys. Rev. D* 76 (2007) 114509. arXiv:0705.3814,
- [12] C. Bonati, M. D’Elia, M. Mariti, M. Mesiti, F. Negro, F. Sanfilippo, Curvature of the chiral pseudocritical line in QCD: Continuum extrapolated results, *Phys. Rev. D* 92 (5) (2015) 054503. arXiv:1507.03571,
- [13] R. Bellwied, et al, The QCD phase diagram from analytic continuation, *Phys. Lett. B* 751 (2015) 559–564. arXiv:1507.07510,
- [14] M. D’Elia, G. Gagliardi, F. Sanfilippo, Higher order quark number fluctuations via imaginary chemical potentials in  $N_f = 2 + 1$  QCD, *Phys. Rev. D* 95 (9) (2017) 094503. arXiv:1611.08285,
- [15] J. Gunther, R. Bellwied, S. Borsanyi, Z. Fodor, S. D. Katz, A. Pasztor, C. Ratti, The QCD equation of state at finite density from analytical continuation, *EPJ Web Conf.* 137 (2017) 07008. arXiv:1607.02493,
- [16] Y. Aoki, G. Endrodi, Z. Fodor, S. Katz, K. Szabo, The Order of the quantum chromodynamics transition predicted by the standard model of particle physics, *Nature* 443 (2006) 675–678. arXiv:hep-lat/0611014,
- [17] S. Borsanyi, Z. Fodor, J. N. Guenther, S. K. Katz, K. K. Szabo, A. Pasztor, I. Portillo, C. Ratti, Higher order fluctuations and correlations of conserved charges from lattice QCD, *JHEP* 10 (2018) 205. arXiv:1805.04445,
- [18] P. Cea, et al, Critical line of 2+1 flavor QCD: Toward the continuum limit, *Phys. Rev. D* 93 (1) (2016) 014507. arXiv:1508.07599,
- [19] R. Bellwied, S. Borsanyi, et al, Fluctuations and correlations in high temperature QCD, *Phys. Rev. D* 92 (11) (2015) 114505.
- [20] JUQUEEN: IBM Blue Gene/Q Supercomputer System at the Jülich Supercomputing Centre, Tech. Rep. 1 A1, Jülich Supercomputing Centre, <http://dx.doi.org/10.17815/jlsrf-1-18> (2015).